Membrane Assembly of the Bacteriophage Pf3 Major Coat Protein†

Alexander B. Meijer, Ruud B. Spruijt, Cor J. A. M. Wolfs, and Marcus A. Hemminga*

Laboratory of Molecular Physics, Department of Biomolecular Sciences, Wageningen University and Research Center, Dreijenlaan 3, 6703 HA Wageningen, The Netherlands

Received December 28, 1999; Revised Manuscript Received March 13, 2000

ABSTRACT: The Pf3 major coat protein of the Pf3 bacteriophage is stored in the inner membrane of the infected cell during the reproductive cycle. The protein consists of 44 amino acids, and contains an acidic amphipathic N-terminal domain, a hydrophobic domain, and a short basic C-terminal domain. The mainly α-helical membrane-bound protein traverses the membrane once, leaving the C-terminus in the cytoplasm and the N-terminus in the periplasm. A cysteine-scanning approach was followed to measure which part of the membrane-bound Pf3 protein is inside or outside the membrane. In this approach, the fluorescence probe *N*-[(iodoacetyl)amino]ethyl-1-sulfonaphthylamine (IAEDANS) was attached to single-cysteine mutants of the Pf3 coat protein. The labeled mutant coat proteins were reconstituted into the phospholipid DOPC/DOPG (80/20 molar ratio) and DOPE/DOPG (80/20 molar ratio) model membranes. We subsequently studied the fluorescence characteristics at the different positions in the protein. We measured the local polarity of the environment of the probe, as well as the accessibility of the probe to the fluorescence quencher acrylamide. The results of this study show a single membrane-spanning protein with both the C- and N-termini remaining close to the surface of the membrane. A nearly identical result was seen previously for the membrane-bound M13 coat protein. On the basis of a comparison between the results from both studies, we suggest an "L-shaped" membrane-bound model for the Pf3 coat protein. DOPE-containing model membranes revealed a higher polarity, and quenching efficiency at the membrane/water interface. Furthermore, from the outside to the inside of the membrane, a steeper polarity gradient was measured at the PE/PG interface as compared to the PC/PG interface. These results suggest a thinner interface for DOPE/DOPG than for DOPC/DOPG membranes.

The subject of this paper is the membrane-bound Pf3 major coat protein of the filamentous bacteriophage Pf3, which specifically infects *Pseudomonas aeruginosa* (*1*). Pf3 bacteriophage belongs to the family Inoviridae, whose members all share structural and biological features. Despite striking similarities in life-cycle processes and structural aspects, the degree of sequence homology of the involved proteins can be low (*2*). Among the best studied filamentous phages are the M13, fd, and Pf1 bacteriophages.

The flexible rodlike bacteriophages consist of single-stranded DNA encapsulated by a tubular protein coat. The most abundant protein in this coat is the gene VIII product, which is called the major coat protein. A few copies of minor coat proteins can be found at the tips [for a recent review, see Marvin et al. (*3*)]. The coat of the Pf3 bacteriophage consists of about 2500 copies of Pf3 major coat protein [for specific construction details, see Welsh et al. (*4*)]. During the reproductive cycle, the major coat protein is stripped from the viral DNA, and stored in the inner membrane of the cell. New major coat proteins are synthesized without a leader sequence, and insert Sec independently into the membrane. The protein traverses the membrane once, leaving the C-terminus in the cytoplasm and the N-terminus in the periplasm (*5*, *6*).

The biological aspects of the filamentous bacteriophage life cycle have been studied for several years as model systems for a wide range of complicated biological processes and interactions. A number of processes from the bacteriophage life cycle serve as models for protein−membrane interactions, macromolecular assembly, and protein−DNA interactions.

In our group, we are interested in two different aspects of the membrane-bound Pf3 major coat protein. First is the structure−function relationship of the membrane-bound Pf3 major coat protein with respect to the Pf3 bacteriophage life cycle. To understand this relation, we needed information about the topology and conformation of the membrane-bound protein. Second, because of its relative simplicity, the protein is an excellent model for studying fundamental aspects of protein−lipid interactions in detail. Topics of interest are, for example, protein insertion into the membrane, anchoring interactions of proteins with the membrane, and the preferred location of specific amino acids in a phospholipid bilayer.

When the first aspect mentioned above is considered, it turns out that only limited structural information is available about the membrane-bound Pf3 major coat protein. The protein consists of 44 amino acids (*7*, *8*), in which three domains can be distinguished: a basic C-terminal domain, a hydrophobic domain, and an acidic amphipathic N-terminal

† This research was supported by the Life Sciences Foundation (SLW) with financial aid of The Netherlands Organization for Scientific Research (NWO).

* To whom correspondence should be addressed. Telephone: 31-317-482044. Fax: 31-317-482725. E-mail: marcus.hemminga@virus.mf.wau.nl.

10.1021/bi992972t CCC: $19.00 © 2000 American Chemical Society
Published on Web 04/27/2000

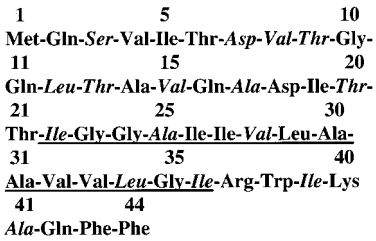

FIGURE 1: Primary structure of the Pf3 major coat protein (*7*, *8*). The hydrophobic domain is underlined. The amino acid residues that were replaced with cysteines in the single-cysteine mutants are in italic. In one of the mutants, a cysteine was placed at the C-terminal end of the protein.

domain (Figure 1). The membrane-bound protein mainly adopts an α-helical conformation. Results from infrared spectroscopy and circular dichroism exhibited an α-helical content of about 75% for the membrane-bound Pf3 major coat protein (*9*).

To obtain more knowledge about the structure of the Pf3 coat protein, a comparison can be made with the M13 and Pf1 major coat protein, because much more information is available about these proteins. M13 and Pf1 major coat protein have been extensively studied in detergent micellar and phospholipid model systems. Like the Pf3 major coat protein, the primary structures of the M13 (*10*) and Pf1 (*11*) major coat protein reveal a basic C-terminal domain, an acidic amphipathic N-terminal domain and a hydrophobic domain. Biophysical techniques (e.g., NMR) showed two α-helical segments, connected with a flexible linker, in detergent-bound M13 (*12*) and Pf1 (*13*) coat protein. These (and other) studies resulted in an "L-shaped" model structure of the M13 and Pf1 major coat proteins in the membrane. One helix spans the membrane, and the second N-terminal amphipathic helix is parallel to the membrane surface (*13*−*15*). As the structural features between the Pf3, M13, and Pf1 bacteriophages are similar, it is interesting to ascertain whether this is also true for both membrane-bound major coat proteins, even though there is no primary sequence homology.

Furthermore, our aim is to study which part of the protein is inside or outside the membrane to obtain membrane-anchoring information. These interactions can be important for many processes, e.g., membrane assembly, topology, and protein insertion (*16*). Anchoring can be accomplished by several factors. The first is by hydrophobic interactions with the phospholipid tails that will be mainly determined by the length of the transmembrane helix. The α-helices generally contain 20 amino acids or more, and consist of highly nonpolar residues. The Pf3 major coat protein has a stretch of 15 hydrophobic amino acids, which is rather short for a membrane-spanning protein.

Second, an important factor for anchoring can be the electrostatic interactions between charged amino acid residues and, for example, charged headgroups of phospholipids. Positively charged residues frequently reside in the cytoplasmic space (positive inside rule) (*17*), and are thought to have anchoring interactions with the membrane. Lysine residues can be found well inside the membrane, leaving the charged amino group in the membrane/water interface as was found for the M13 coat protein (*18*, *19*) which is called the "snorkeling effect" (*20*). There are two positively charged residues in the C-terminus of the Pf3 protein. Therefore, we are interested in determining whether this snorkeling effect occurs in this protein.

Third, important for anchoring are also the aromatic amino acid residues (*21*). Tryptophan residues are often found near the membrane/water interface (*22*−*25*), although the mechanism for this interaction is not fully understood. The Pf3 major coat protein contains a tryptophan residue in the C-terminus and two phenylalanines at the very end. Therefore, the protein is an excellent model for studying the location of those residues.

To study the above-mentioned aspects, membrane-bound Pf3 coat protein was studied with site-specific probing, as was described for the M13 coat protein, bacteriorhodopsin, and colicin (*26*−*29*). For this purpose, we prepared mutants such that single cysteines were present and regularly spaced along the primary structure of the protein. The fluorescence probe IAEDANS[1] was specifically attached to the cysteine residue. The labeled mutant coat proteins are subsequently reconstituted into phospholipid model systems, and we studied the fluorescence characteristics of the probe at the specific positions. One of these characteristics was the sensitivity of the probe to the polarity of the environment (*30*). The quenching efficiency was also measured using the polar quencher acrylamide. In this way, information is obtained about the depth of amino acids with respect to the membrane. This information supports an L-shaped membrane assembly of the Pf3 coat protein, as was found for the membrane-bound M13 and Pf1 coat proteins.

MATERIALS AND METHODS

Chemicals. The phospholipids dioleoylphosphatidylcholine (DOPC) and dioleoylphosphatidylglycerol (DOPG) were obtained from Sigma. Dioleoylphosphatidylethanolamine (DOPE) was purchased from Avanti. Other fine chemicals were from Merck.

Preparation of Cysteine Mutants. The pT7-7 plasmid with the Pf3 major coat protein gene as an insert (pT7-7p44) was a generous gift from A. Kuhn (Department of Microbiology, University of Hohenheim, Stuttgart, Germany). For details of the construction of this plasmid, see Kiefer et al. (*6*). Site-specific cysteine mutants were prepared with the QuikChange Site-Directed Mutagenisis Kit from Stratagene. The oligonucleotides used in this procedure were purchased from Amersham Pharmacia Biotech. The sequence of the mutant DNA was verified using automated DNA sequencing. Correctly mutated plasmid DNA was transformed into competent *Escherichia coli* BL21(DE3) cells (*31*).

Overexpression of Pf3 Major Coat Protein. E. coli BL21-(DE3) with plasmid pT7-7p44 was grown at 37 °C to an optical density at 600 nm of about 0.7, under continuous shaking and aeration in an 8 L LB culture [containing 0.5% (w/v) yeast extract, 1% (w/v) tryptone, 1% (w/v) NaCl, 0.2% (w/v) glucose, and 0.01% (w/v) ampicillin]. The cells were induced with isopropyl β-D-thiogalactopyranoside (final

[1] Abbreviations: IAEDANS, [*N*-(iodoacetyl)amino]ethyl-1-sulfonaphthylamine; DOPC, dioleoylphosphatidylcholine; DOPG, dioleoylphosphatidylglycerol; DOPE, dioleoylphosphatidylethanolamine; TFE, trifluoroethanol; HPSEC, high-performance size-exclusion chromatography; *L*/*P*, lipid to protein molar ration; DTT, dithiothreitol; SDS, sodium dodecyl sulfate; λ_{max}, wavelength of maximum emission; K_{sv}, Stern−Volmer constant.

concentration of 0.15 mM). One hour after induction, the cells were harvested by centrifugation at 7000*g* for 10 min at 4 °C. The cells were resuspended in 150 mL of lysis buffer [137 mM NaCl, 2.7 mM KCl, 25 mM Tris-HCl, 1 mM DTT, and 1 mM PMSF (pH 7.5)] and sonicated on ice with a Branson B15 cell disrupter (90 W, 6 min, 50% duty cycle). The membrane fraction was collected by centrifugation for 30 min at 29 500 rpm in a 60Ti rotor using a Beckman XL-90 ultracentrifuge. The membrane fraction was finally resuspended in 8 mL of lysis buffer and stored at −20 °C. Samples of the overexpressed single-cysteine mutants were analyzed with Tricine SDS−polyacrylamide gel electrophoresis (*32*).

Purification and Labeling of the Pf3 Major Coat Protein. To extract the protein from the membrane, 5 mL of the resuspended membrane fraction, from the procedure described above, was thawed and mixed with 5 mL of TFE. Membrane proteins were collected in the supernatant after the remaining membrane debris had been removed by centrifugation at 17 000 rpm in a MSE 8 × 50 rotor (20 °C). The extract proved to be unstable in time. Therefore, it was immediately loaded (2 × 5 mL of protein extract) onto a Source 15 RPC reversed phase column (1 × 10 cm, Pharmacia Biotech) running in 20% (v/v) 2-propanol and 0.1% (v/v) triethylamine with a flow rate of 1 mL/min. Immediately after loading was complete, a 2-propanol/water gradient was started by keeping the concentration of triethylamine at a constant level of 0.1% (v/v). Triethylamine proved to be crucial for releasing the coat proteins from the column. The following gradient was used: from 0 to 5 min, 20 to 35% 2-propanol; from 15 to 50 min, 35 to 70% 2-propanol; and from 50 to 55 to 60 min, 70 to 100 to 20% 2-propanol.

After reversed phase chromatography, a fraction of about 80% pure Pf3 coat protein was collected and diluted (1/1 v/v) with TFE. In the following step, 2 mg of IAEDANS (Molecular Probes) was added to the protein fraction in the presence of 1.6% (v/v) tributylphosphine (Fluka Chemie). The reducing agent tributylphosphine was selected because it does not interfere with the reaction between IAEDANS and the thiol group of the cysteine residue (*33*). The fluorescence probe was allowed to react (in the dark) with the cysteine's thiol group of the mutant coat protein for 3 h under continuous stirring at room temperature. The labeling reaction was stopped with an excess of DTT. At the end of the reaction, the detergent cholate was added to the mixture (final concentration of 50 mM).

In the next step, unbound label and remaining impurities were separated from the labeled major coat protein by HPSEC using a Superdex75 prep-grade column (HR 16/50) running in 50 mM sodium cholate, 1 mM EDTA, 150 mM NaCl, and 10 mM Tris-HCl (pH 8) at a flow rate of 1 mL/min. Volumes (2 mL) of the reaction mixture were loaded on the column. The presence of TFE in the reaction mixture was essential for the success of the purification procedure. The retention time of the Pf3 coat protein on the Superdex 75 column was prolonged by 5 min. This resulted in a higher efficiency in size separation and, therefore, a better removal of the remaining larger proteins. This observation suggests a decrease in the aggregational size of the coat proteins in the presence in TFE.

After size-exclusion chromatography, fractions of about 95% pure labeled Pf3 protein (assessed by Tricine SDS−polyacrylamide gel electrophoreses) were pooled, and concentrated using ultrafiltration over an Amicon YM10 membrane. The pure labeled mutant protein was finally stored at −20 °C. The final concentration of the purified protein depended on which mutant was purified because the initial level of expression was an important factor in the final yield of the protein. The concentration of protein varied between 2 and 20 μg/mL. Because of the absence of a cysteine amino acid residue, we could not label the wild-type protein with this procedure. This result showed a high level of specificity in the labeling reaction between IAEDANS and the cysteine residues in the mutant coat proteins.

Reconstitution into Phospholipid Model Membranes. Labeled Pf3 major coat protein was reconstituted into DOPC/DOPG (80/20 molar ratio) and DOPE/DOPG (80/20 molar ratio) using the cholate dialysis method (*34*). The amount of phospholipids was chosen such that the lipid/protein molar ratio (*L*/*P*) was above 250. Chloroform was evaporated from the desired amount of phospholipid solution, and the residual traces of chloroform were removed by drying under vacuum for at least 2 h. The lipids were subsequently solubilized in 50 mM cholate, 1 mM EDTA, 150 mM NaCl, and 10 mM Tris-HCl (pH 8) and mixed with the labeled protein. In the following step, the lipid/protein mixture was dialyzed for 60 h against a 1000-fold excess of buffer containing 1 mM EDTA, 150 mM NaCl, and 10 mM Tris-HCl (pH 8). The buffer was replaced every 12 h. Typically, samples for the steady-state fluorescence measurements contained about 0.9 mg of phospholipids.

Steady-State Fluorescence. Samples (1 mL) of every reconstituted mutant in DOPC/DOPG (80/20) and DOPE/DOPG (80/20) membranes were prepared for the steady-state fluorescence experiment. The background samples contained DOPC/DOPG (80/20) and DOPE/DOPC (80/20) with and without the wild-type protein. Fluorescence spectra of the labeled mutants were collected at 22 ± 0.5 °C using an excitation wavelength of 340 nm on a SPEX Fluorolog 3-22 fluorometer equipped with a 450 W xenon lamp as an excitation source. Excitation and emission bandwidths were set to 1 and 3 nm, respectively, and spectra were recorded between 400 and 600 nm with an integration time of 0.5 s. Samples (1 mL) were in 1 cm light path fused silica cuvettes (Hellma model 114F-QS), and the optical density at 340 nm never exceeded 0.1. The spectra were corrected for the background signal and sensitivity of the photomultiplier.

For steady-state fluorescence quenching experiments, aliquots of an acrylamide stock solution [3 M acrylamide, 150 mM NaCl, 10 mM Tris-HCl, and 1 mM EDTA (pH 8)] were added to samples of labeled protein reconstituted in DOPC/DOPG (80/20) and DOPE/DOPG (80/20) membranes after the steady-state fluorescence experiments. After every addition of acrylamide (steps of 5 or 10 μL to a final concentration of 176 mM), the decrease in fluorescence intensity was measured. Appropriate corrections for dilution were made for these quenching experiments.

The fluorescence data were analyzed according to the Stern−Volmer equation for collisional quenching (*35*, *36*):

$$\frac{F_0}{F} = 1 + K_{sv}[Q]$$

with

$$K_{sv} = k_q \tau$$

where F_o and F are the fluorescence intensities in the absence and presence of the quencher Q, respectively. K_{sv} is the Stern−Volmer quenching constant. It equals the fluorescence lifetime (τ) times the accessibility constant k_q. Before and after the fluorescence experiments, the aggregational state of the protein was checked by HPSEC as described by Spruijt et al. (*37*).

RESULTS

Preparation of Single-Cysteine Mutants. Seventeen single-cysteine mutants of the Pf3 major coat protein were prepared to ensure the presence of a cysteine residue well spread along the primary structure of the protein (see Figure 1). One of these mutant coat proteins contained an additional cysteine residue at the C-terminal end of the protein.

The level of expression in *E. coli* was reduced by a factor of 10 in most single-cysteine mutants, as compared to the level of expression of the wild-type protein. Replacement of the amino acids at positions 8 and 12 resulted in a dramatic decrease in the level of expression, and those mutants could not be purified in sufficient amounts for the fluorescence experiments. Interestingly, the three threonine residues in the N-terminus at positions 9, 13, and 20 could be replaced without any decrease in the expression level. In contrast, all cell cultures producing mutant coat proteins exhibited a comparable growth pattern. First, the optical density at 600 nm of the cell culture increased to about 0.7. After induction of the target protein synthesis, the optical density decreased slightly, and reached a constant value of about 0.6.

After collection and fractionation of the cells, Pf3 major coat protein mutants were predominantly (about 95%) found in the membrane fraction. Incorrectly inserted protein is probably rapidly degraded by cell protease activity. It is difficult to assess the reason for the decrease in the level of expression of coat protein mutants, because a large number of cellular processes are involved in protein synthesis and membrane insertion. For instance, the production of the protein might be inhibited on the DNA level, resulting in a lower level of expression. On the other hand, perhaps the membrane insertion process is slowed or even blocked because of the replacement of a specific amino acid residue by a cysteine residue.

Steady-State Fluorescence Spectroscopy. The polarity of the environment around the AEDANS probe was measured by steady-state fluorescence spectroscopy. This polarity is reflected in the wavelength of maximum emission, which is specified as λ_{max}. Figure 2 shows the λ_{max} values of the AEDANS probes attached to the different positions in the coat proteins, which were reconstituted into DOPC/DOPG (80/20) and DOPE/DOPG (80/20) membranes. The probe attached to amino acid position 45 has the highest λ_{max} value (500 nm) in DOPC/DOPG membranes, indicating that this position is in the most polar environment. λ_{max} decreases to 481 nm at position 36, and is almost constant between positions 36 and 25. From position 25 to 13, λ_{max} gradually increases to 493 nm. Positions 3, 7, and 9 have a constant emission maximum of 494 nm. A similar trend is observed In DOPE/DOPG membranes. Upon comparison of the results

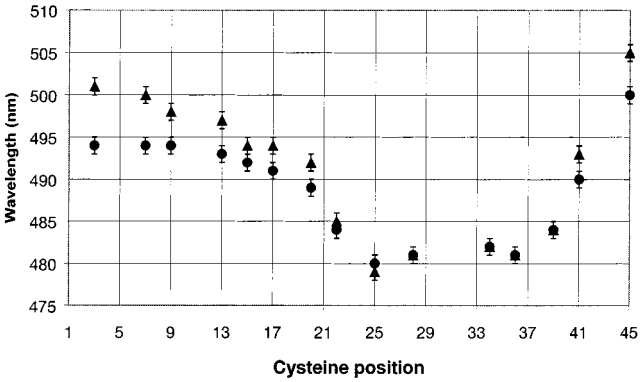

FIGURE 2: Polarity plot of the labeled Pf3 major coat protein. The wavelength of maximum emission, λ_{max}, of AEDANS is plotted as a function of the cysteine position to which the probe is attached with (●) labeled mutant coat proteins reconstituted in DOPC/DOPG (80/20) membranes and (▲) labeled mutant coat proteins reconstituted in DOPE/DOPG (80/20) membranes.

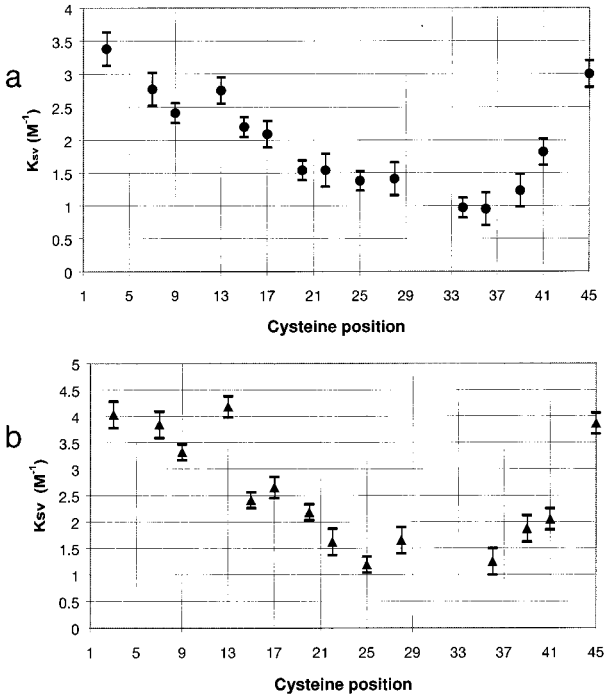

FIGURE 3: Fluorescence quenching plot. The Stern−Volmer constant, K_{sv}, as a function of the position to which the probe is attached with (a) labeled mutant coat proteins reconstituted in DOPC/DOPG (80/20) membranes (●) and (b) labeled mutant coat proteins reconstituted in DOPE/DOPG (80/20) membranes (▲).

obtained for both DOPC/DOPG and DOPE/DOPG membranes, a difference can be seen in λ_{max} at N- and C-terminal positions of the protein. These positions exhibit a higher value of λ_{max} in DOPE/DOPG membranes, suggesting a more polar environment.

After the quenching experiment, Stern−Volmer plots were constructed. The plots showed a nearly linear relation between F_o/F and the acrylamide quencher concentration [Q] (data not shown). The Stern−Volmer constant K_{sv} was determined for all the labeled mutant coat proteins reconstituted in DOPC/DOPG and DOPE/DOPG membranes. Figure 3 shows K_{sv} values for both model systems as a function of the cysteine position to which the probe is attached. In DOPC/DOPG membranes, it can be seen that K_{sv} rapidly decreases from 3 M^{-1} at position 45 to 0.95 M^{-1}

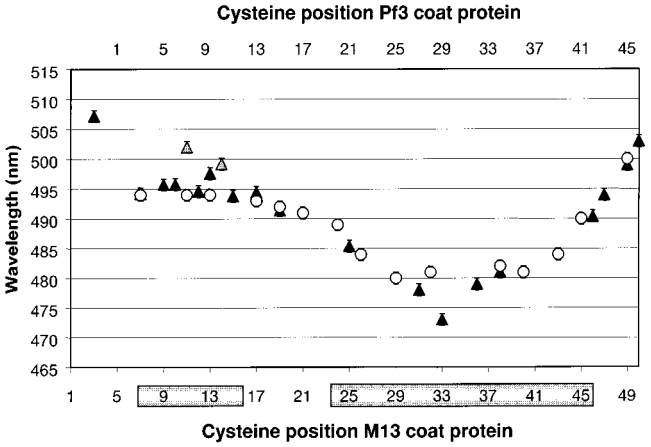

FIGURE 4: Overlay of the polarity plots of the labeled M13 (ref *26* and unpublished experiments) and Pf3 major coat protein reconstituted in DOPC/DOPG (80/20) membranes. The top horizontal axis is the primary structure of the Pf3 coat protein with (○) the Pf3 data points. The bottom horizontal axis is the primary structure of the M13 coat protein (*10*); indicated is the amphipathic helix from residue 7 to 16 and the transmembrane helix from residue 25 to 45 (*12*) with (▲) the M13 data points. Further details about strongly deviating M13 positions 11 and 14 (gray triangles) will be published.

at position 36. When going from position 36 to position 13, we observed a gradual increase in K_{sv} (from 0.95 to 2.75 M^{-1}). K_{sv} decreases slightly at position 9 to 2.41 M^{-1} and increases again to 3.38 M^{-1} at position 3. Again, in DOPE/DOPG membranes, we observed a similar trend in K_{sv} as a function of the positions in the protein. In a comparison of the two model systems in Figure 4, the N- and C-terminal positions clearly have higher K_{sv} values in DOPE/DOPG membranes. Furthermore, the fluctuations in K_{sv} between (especially) N-terminal positions are stronger in DOPE/DOPG membranes than in DOPC/DOPG membranes.

DISCUSSION

L-Shaped Assembly of the Membrane-Bound Pf3 Coat Protein. We determined the location of amino acid residues in the membrane of reconstituted Pf3 major coat protein using site-specific probing. The cysteine residues of the coat protein mutants were regularly spaced along the primary structure of the protein. The mutants are assumed to be similar to the wild-type protein, as we selected and purified mutant proteins from the membrane fraction of *E. coli* cells, thereby minimizing the possibility of isolating misfolded and not inserted protein. Moreover, the chemical and physical behavior of all mutants is equal to that of the wild-type Pf3 coat protein during the purification procedure.

With the fluorescence probe IAEDANS attached to the cysteine residues of the reconstituted mutants, we monitored the polarity of the environment at specific positions of the protein in the membrane. This polarity is reflected in the wavelength of maximum emission (λ_{max}) of the IAEDANS probe (*30*). Probes will have a smaller λ_{max} in the membrane than do probes at the outside. The location of amino acids is also determined with fluorescence quenching. The uncharged polar quencher acrylamide quenches the fluorescence of IAEDANS more efficiently when the probe is in the aqueous phase (*26*, *38*). This will result in a large Stern−Volmer constant (K_{sv}). In contrast, probes in the membrane exhibit a small value. K_{sv} is correlated to the accessibility of the probe to the fluorescence quencher.

Roughly three environments can be distinguished in the membrane (1) a hydrophobic environment between the phospholipid carbon tails, (2) a more polar region in the phospholipid headgroup region (interface), and (3) the most polar region in the water phase. There are no sharp boundaries between these three regions. Wiener and White proposed a model of the structure of L_α-phase DOPC bilayers by interpreting X-ray and neutron diffraction data (*39*). Their model shows a Gaussian distribution of the different membrane components, giving rise to a chemically highly heterogeneous interface. The combined interfacial region is about 50% of the total thickness of the membrane. This leads to a polarity gradient from the outside to the inside of the membrane (*40*).

IAEDANS would ideally reflect this polarity gradient as a symmetrical "cuplike" shape when λ_{max} is measured as a function of membrane depth. A similar symmetrical pattern is expected for the K_{sv} as a function of membrane depth. In contrast, the measured polarity and fluorescence-quenching plot (Figures 2 and 3a,b) exhibit asymmetrical patterns in DOPC/DOPG and DOPE/DOPG membranes. A close examination of these figures reveals a more gradual increase in K_{sv} and λ_{max} at the N-terminal side (positions 25−13) of the protein than at the C-terminal side (positions 34−45). These results suggest that the "simple" model of a Pf3 protein spanning the entire membrane, with the C- and N-termini in the aqueous phase, is not valid.

Upon comparison of both phospholipid systems, a difference in λ_{max} and K_{sv} can be seen at the C- and N-termini. At these positions, the wavelengths of maximal emission are red-shifted, and more efficiently quenched in DOPE/DOPG membranes. We can explain this result by more closely examining the PE headgroup region. The clearly more polar PE headgroup brings a higher polarity to the interface than does the PC headgroup, which subsequently leads to a more red-shifted λ_{max} in DOPE/DOPG membranes. Furthermore, molecular dynamic studies [reviewed in Tieleman et al. (*41*)] showed that the interface is thinner in PE-containing membranes than in PC-containing membranes. Therefore, probes are more accessible to the aqueous quencher (acrylamide) in the PE-containing membrane, resulting in a larger K_{sv}. One would expect that the interfacial differences between both phospholipid systems are no longer observed for positions which are completely in the water phase. However, those positions were not found in this study. Consequently, the C- and N-termini remain in (or are close to) the membrane/water interface. As a consequence of the close proximity of the membrane, λ_{max} at position 45 (505 nm in DOPE/DOPG membranes and 500 nm in DOPC/DOPG membranes) does not reach the wavelength of 520 nm obtained in water (*30*). The conclusion is further supported by the fact that the C-terminus is not accessible to proteases K in topology experiments with Pf3 major coat protein (*6*).

The local environment at a specific position gives rise to a fine structure in the pattern of both the polarity and quenching plot. The presence of, for example, a charged residue near the monitored position increases the local polarity, which is reflected in a slightly higher λ_{max}. The opposite is true for a flanking hydrophobic residue. Efficient fluorescence quenching can be blocked by steric hindrance

of neighboring amino acids (or local tertiary structure), resulting in an unexpected value of K_{sv}. Furthermore, K_{sv} is dependent not only on the accessibility of the probe to the quencher acrylamide but also on the fluorescence lifetime. The lifetime of the probe is longer in an apolar solvent than in a polar solvent (*30*). Therefore, the differences are smaller in the actual accessibility of the fluorescence probe as a function of the position. This also explains the variations in fine structure that occur between the polarity and quenching plot.

The variation between K_{sv} and λ_{max}, giving rise to the fine structure, appears to be stronger in DOPE/DOPG membranes. A possible explanation for this effect could be the thinner interfacial region in DOPE/DOPG membranes as compared to that in DOPC/DOPG membranes. This leads to a much steeper polarity gradient in the DOPE/DOPG interface. Small shifts in the position of the probe in the interface can subsequently give rise to stronger variations in K_{sv} and λ_{max} as a function of the position in the protein.

Spruijt et al. (*26*) measured the relative depth of amino acids of the M13 major coat protein in a membrane using an approach that was identical to that used in this study for the Pf3 major coat protein. Information about the local polarity of the environment was obtained for positions in the transmembrane helix and the C-terminus. Because of a different instrumental setup in the measurements of that study, the wavelength of maximum emission was about 10 nm too low for all the positions (the scanning approach was repeated for these positions). At this moment, information about the polarity of the environment is also available for the N-terminal positions of the reconstituted M13 major coat protein in DOPC/DOPG membranes (80/20) (unpublished experiments).

A striking similarity can be seen in the shape of the polarity plots of both the Pf3 and M13 membrane-bound coat proteins (Figure 4). We aligned the positions in the primary structure of both proteins such that the environments of the different positions match in polarity. The above-mentioned alignment of the polarity plot clearly indicates a strong similarity in the depth of the amino acid positions of the M13 and Pf3 coat protein. Even the replacement of the charged residue at position 7 of the Pf3 coat protein did not result in a strong deviation between the results of both proteins. N-Terminal positions 3, 11, and 14 of the M13 coat protein deviate from the other positions. Position 3 is part of the unstructured N-terminal end of the M13 protein, and is probably in the aqueous phase. The substitutions of membrane-anchoring amino acids phenylalanine 11 and leucine 14 result in a rearrangement of the N-terminal arm with respect to the surface of the membrane. Further details about these amino acids will be published. The similarity observed in Figure 4 is a strong indication for a structural resemblance between both proteins. This is remarkable taking into account the lack of primary sequence homology.

Much structural information is available about the membrane-bound M13 coat protein. A model, proposed for the membrane-bound M13 coat proteins, exhibits an L-shaped membrane-bound assembly. A transmembrane helix, which is perpendicular to the membrane surface, is connected by a flexible linker or loop to an amphipathic α-helix that is parallel to the membrane surface (*14*, *15*, *42*). Much less information is available about the membrane-bound Pf3 coat protein. It is known that it predominantly contains an α-helical structure (*9*). Like the M13 coat protein, an amphipathic α-helix can be constructed of the N-terminus (*43*). The striking similarity between the polarity plots (Figure 4) of both proteins strongly suggests the presence of an L-shape in the membrane-bound Pf3 coat protein. The asymmetrical shape of both the polarity and quenching plot (Figures 2 and 3a) is a direct result of this protein topology. The presence of the loop structure or flexible linker can explain the result of a more gradual increase in K_{sv} and λ_{max} at the N-terminal side of the protein from position 25 to 13.

It is a tenuous prospect to extract more information from the above-mentioned alignment between M13 and Pf3 coat protein (Figure 4 also shows the assignment of the structural domains of the M13 coat protein). The limited structural information about the Pf3 coat protein makes it difficult to assign the amino acids to structural domains. On the basis of the alignment, we could speculate that the amphipathic helix of the membrane-bound Pf3 coat is approximately between amino acids 3 and 12 followed by a loop or linker between positions 14 and 20 that is subsequently connected to the transmembrane helix.

Relative Depths of C-Terminal Amino Acid Residues in the Membrane. The primary structure of the Pf3 coat protein contains an arginine at position 37 and a lysine at position 40. Two phenylalanines (positions 43 and 44) are at the C-terminal end of the protein (Figure 1). One would expect to find both charged residues at the polar interface, and the two phenylalanines in the hydrophobic region of the membrane. This would form a tight anchor between the C-terminus and the membrane.

A closer examination of the polarity and quenching plot (Figures 2 and 3a,b) is required to determine the location of those amino acids in the membrane. In our experimental approach, it is not possible to measure the absolute depth with respect to the membrane surface. There is no reference value for λ_{max} and K_{sv} of probes (attached to the protein) in the water phase that can be used as a starting point from which we can deduce the depth of the amino acids. Nevertheless, on a relative scale, probed positions 36 and 39 can be used to provide information about the relative location of arginine 37 and lysine 40. Position 45 can be used to monitor the location of both phenylalanines.

Positions 36 and 39 exhibit small K_{sv} and λ_{max} compared to those of position 45. This result suggests a deeper penetration of the charged residues in the membrane than both phenylalanines. Probably, the Cα backbone of the amino acid side chains (at least arginine 37) is in the hydrophobic part of the membrane with the charged group sticking out in the polar interface [the snorkeling effect (*18*, *20*)]. A similar result was found for the lysine residues at positions 40, 43, and 44 of the M13 coat protein with ESR and fluorescence studies (*19*, *26*).

Contrary to the suggestion following from the results (a high value of K_{sv} and λ_{max} at position 45), it is still possible that the phenylalanines bend back to the hydrophobic part of the membrane. This can be explained as follows. The AEDANS probe at the outer C-terminus encounters only one neighboring amino acid. This reduces the amount of steric hindrance, and might give the probe enough freedom to reach for the outside of the membrane. If both residues are indeed located in the interface, additional (unknown) interactions

of the phenylalanines with the interfacial region are to be expected. Perhaps both phenylalanines have the ability to form a π-stack, or cation-π interactions (*44*) play a role in stabilizing the phenylalanines in the interface.

Conclusions. The location of amino acids of Pf3 mutants in the membrane, as studied by site-specific fluorescence probing, shows a single membrane-spanning protein with both the C- and N-termini remaining close to the surface of, or are in, the membrane. Unfortunately, it was only possible to obtain relative locations of the amino acids in the membrane. A comparison with a similar study performed on the M13 coat protein reveals striking similarities. The structural coherence that follows from this comparison suggests an L-shaped tertiary structure of the membrane-bound Pf3 coat protein. A similar model was also proposed for the membrane-bound Pf1 coat protein. It appears that not only the mechanisms in viral reproduction but also the structure of the involved major coat proteins are comparable. A higher polarity was detected in the interface of PE/PG membranes than in PC/PG membranes. Furthermore, the PE/PG interface appears to have a steeper polarity gradient than the PC/PG headgroup region, upon going from the outside to the inside of the membrane. This follows directly from a smaller interfacial region, and a more polar headgroup region of DOPE/DOPG membranes as compared to DOPC/DOPG membranes.

ACKNOWLEDGMENT

We acknowledge Prof. Dr. A. Kuhn (Department of Microbiology, University of Hohenheim) for the generous gift of the plasmid containing the Pf3 major coat protein gene.

REFERENCES

1. Stanisich, V. A. (1974) *J. Gen. Microbiol. 84*, 332−342.
2. Russel, M. (1991) *Mol. Microbiol. 5*, 1607−1613.
3. Marvin, D. A. (1998) *Curr. Opin. Struct. Biol. 8*, 150−158.
4. Welsh, L. C., Symmons, M. F., Sturtevant, J. M., Marvin, D. A., and Perham, R. N. (1998) *J. Mol. Biol. 283*, 155−177.
5. Kuhn, A., Rohrer, J., and Gallusser, A. (1990) *J. Struct. Biol. 104*, 38−43.
6. Kiefer, D., Hu, X., Dalbey, R., and Kuhn, A. (1997) *EMBO J. 16*, 2197−2204.
7. Luiten, R. G. M., Schoenmakers, J. G. G., and Konings, R. N. H. (1983) *Nucleic Acids Res. 11*, 8073−8085.
8. Putterman, D. G., Casadevall, A., Boyle, P. D., Yang, H. L., Frangione, B., and Day, L. A. (1984) *Proc. Natl. Acad. Sci. U.S.A. 81*, 699−703.
9. Thiaudiere, E., Soekarjo, M., Kuchinka, E., Kuhn, A., and Vogel, H. (1993) *Biochemistry 32*, 12186−12196.
10. Van Wezenbeek, P. M. G. F., Hulsebos, T. J. M., and Schoenmakers, J. G. G. (1980) *Gene 11*, 129−148.
11. Nakashima, Y., Wiseman, R. L., Konigsberg, W., and Marvin, D. A. (1975) *Nature 253*, 68−71.
12. Papavoine, C. H. M., Christiaans, B. E. C., Folmer, R. H. A., Konings, R. N. H., and Hilbers, C. W. (1998) *J. Mol. Biol. 282*, 401−419.
13. Shon, K. J., Kim, Y. G., Colnago, L. A., and Opella, S. J. (1991) *Science 252*, 1303−1304.
14. McDonnell, P. A., Shon, K., Kim, Y., and Opella, S. J. (1993) *J. Mol. Biol. 233*, 447−463.
15. Marassi, F. M., Ramamoorthy, A., and Opella, S. J. (1997) *Proc. Natl. Acad. Sci. U.S.A. 94*, 8551−8556.
16. Killian, J. A. (1998) *Biochim. Biophys. Acta 1376*, 401−416.
17. von Heijne, G., and Gavel, Y. (1988) *Eur. J. Biochem. 174*, 671−678.
18. Tanford, C., and Reynolds, J. A. (1976) *Biochim. Biophys. Acta 457*, 133−170.
19. Stopar, D., Jansen, K. A. J., Pali, T., Marsh, D., and Hemminga, M. A. (1997) *Biochemistry 36*, 8261−8268.
20. Mishra, V. K., Palgunachari, M. N., Segrest, J. P., and Anantharamaiah, G. M. (1994) *J. Biol. Chem. 269*, 7185−7191.
21. Killian, J. A., Salemink, I., Deplanque, M. R. R., Lindblom, G., Koeppe, R. E., and Greathouse, D. V. (1996) *Biochemistry 35*, 1037−1045.
22. Doyle, D. A., Cabral, J. M., Pfuetzner, R. A., Kuo, A., Gulbis, J. M., Cohen, S. L., Chait, B. T., and MacKinnon, R. (1998) *Science 280*, 69−77.
23. Ostermeier, C., Iwata, S., and Michel, H. (1996) *Curr. Opin. Struct. Biol. 6*, 460−466.
24. Reithmeier, R. A. (1995) *Curr. Opin. Struct. Biol. 5*, 491−500.
25. von Heijne, G. (1994) *Annu. Rev. Biophys. Biomol. Struct. 23*, 167−192.
26. Spruijt, R. B., Wolfs, C. J. A. M., Verver, J. W. G., and Hemminga, M. A. (1996) *Biochemistry 35*, 10383−10391.
27. Flitsch, S. L., and Khorana, H. G. (1989) *Biochemistry 28*, 7800−7805.
28. Altenbach, C., Flitsch, S. L., Khorana, H. G., and Hubbell, W. L. (1989) *Biochemistry 28*, 7806−7812.
29. Lakey, J. H., Baty, D., and Pattus, F. (1991) *J. Mol. Biol. 218*, 639−653.
30. Hudson, E. N., and Weber, G. (1973) *Biochemistry 12*, 4154−4161.
31. Studier, F. W., Rosenberg, A. H., Dunn, J. J., and Dubendorf, J. W. (1990) *Methods Enzymol. 185*, 60−89.
32. Schägger, H., and Von Jagow, G. (1987) *Anal. Biochem. 166*, 368−379.
33. Rüegg, U. T., and Rudinger, J. (1977) *Methods Enzymol. 47*, 111−114.
34. Spruijt, R. B., Wolfs, C. J. A. M., and Hemminga, M. A. (1989) *Biochemistry 28*, 9158−9165.
35. Lehrer, S. S. (1971) *Biochemistry 10*, 3254−3263.
36. Lehrer, S. S., and Leavis, P. C. (1978) *Methods Enzymol. 49*, 222−236.
37. Spruijt, R. B., and Hemminga, M. A. (1991) *Biochemistry 30*, 11147−11154.
38. Moro, F., Goni, F. M., and Urbaneja, M. A. (1993) *FEBS Lett. 330*, 129−132.
39. Wiener, M. C., and White, S. H. (1992) *Biophys. J. 61*, 437−447.
40. White, S. H., Wimley, W. C., Ladokhin, A. S., and Hristova, K. (1998) *Methods Enzymol. 295*, 62−87.
41. Tieleman, D. P., Marrink, S. J., and Berendsen, H. J. C. (1997) *Biochim. Biophys. Acta 1331*, 235−270.
42. Papavoine, C. H. M., Remerowski, M. L., Horstink, L. M., Konings, R. N. H., Hilbers, C. W., and van de Ven, F. J. M. (1997) *Biochemistry 36*, 4015−4026.
43. Kishchenko, G., and Makowski, L. (1997) *Proteins: Struct., Funct., Genet. 27*, 405−409.
44. Dougherty, D. A. (1996) *Science 271*, 163−168.

BI992972T